Optik - International Journal for Light and Electron Optics 173 (2018) 263–270

Contents lists available at ScienceDirect

Optik

journal homepage: www.elsevier.com/locate/ijleo

Original research article

Magneto-optical absorption in quantum dot via two-photon absorption process

Doan Q. Khoa[a,b], Nguyen N. Hieu[c], Tran N. Bich[d], Le T.T. Phuong[e], Bui D. Hoi[e], Tran P.T. Linh[f], Quach K. Quang[g], Chuong V. Nguyen[h,*], Huynh V. Phuc[i,*]

[a] Division of Computational Physics, Institute for Computational Science, Ton Duc Thang University, Ho Chi Minh City, Viet Nam
[b] Faculty of Electrical and Electronics Engineering, Ton Duc Thang University, Ho Chi Minh City, Viet Nam
[c] Institute of Research and Development, Duy Tan University, Da Nang 550000, Viet Nam
[d] Division of Physics, Quang Binh University, Quang Binh 510000, Viet Nam
[e] Center for Theoretical and Computational Physics, University of Education, Hue University, Hue 530000, Viet Nam
[f] Faculty of Physics, Hanoi National University of Education, 136 Xuan Thuy, Cau Giay, Ha Noi 100000, Viet Nam
[g] International Cooperation Department, Dong Thap University, Dong Thap 870000, Viet Nam
[h] Department of Materials Science and Engineering, Le Quy Don Technical University, Ha Noi 100000, Viet Nam
[i] Division of Theoretical Physics, Dong Thap University, Dong Thap 870000, Viet Nam

ARTICLE INFO

Keywords:
Magneto-optical absorption
Quantum dot
Two-photon process
E–p interaction
FWHM

ABSTRACT

The magneto-optical absorption coefficients (MOAC) and the full-width at half-maximum (FWHM) in a quasi-zero-dimensional quantum dot (QD) via two-photon process are theoretically studied in which the electron–phonon (e–p) interaction is involved. It is found that the best range of the magnetic field to observe the MOAC is from $B = 3.49$ T to $B = 15.77$ T. As the magnetic field enhances, the peaks intensities firstly enhance, reach the maximum value at $B = 5.38$ T, and then start reducing if the magnetic field continues increases further, while the peaks positions give a blue-shift. Besides, the magneto-optical absorption properties are found to be significantly affected not only by the quantum dot parameter but also by the temperature. The FWHM rises nonlinearly with the enhance of the magnetic field, the confinement frequency, and the temperature. The two-photon process makes an appreciable amount of the total absorption process.

1. Introduction

Because of its high potentials in optoelectronic device applications [1–4], the linear and nonlinear optical properties in low-dimensional semiconductors systems have attracted considerable interest by many scientists in recent years. Among these properties, researches have paid attention to the nonlinear optical rectification [5–8], the second and third-order nonlinear susceptibility [9–11], the second (SHG) [12–14], the third-harmonic generation (THG) [15–19], and the optical absorption coefficients (OACs) [8,20–23]. Their reports show that the optical properties of such systems are powerfully affected and therefore can be controlled by changing the characteristics such as the size or the shapes of the systems. Besides, it is indicated that the increase of the number of the confinement dimension, i.e., the transferring from the three dimensional systems to the quasi-zero dimensional system quantum dots increases the quantum confinement effect, and therefore enhanced their optical properties.

To be typical zero-dimensional systems, semiconductor quantum dots (QD) with different potential shapes have been being investigated in recent decades due to their wonderfully potential applications in the areas of electronics and optics. In a report about

* Corresponding author.
E-mail addresses: doanquockhoa@tdtu.edu.vn (D.Q. Khoa), chuong.vnguyen@lqdtu.edu.vn (C.V. Nguyen), hvphuc@dthu.edu.vn (H.V. Phuc).

https://doi.org/10.1016/j.ijleo.2018.08.030
Received 4 June 2018; Accepted 13 August 2018
0030-4026/ © 2018 Elsevier GmbH. All rights reserved.

the optical absorption in a lens shape QD, Bouzaiene et al. [24] demonstrated that the energy levels as well as the total OAC peaks position are strongly affected not only by the applied hydrostatic pressure, the quantum dot size, and the temperature, but also by the applied electric field. Liu et al. discussed the optical properties of the disk-shaped QD [25], in which the confinement potential is combined by the parabolic and hyperbolic ones. Solving in details the Schrödinger equation, they obtained the electron eigenfunction and its corresponding eigenvalue explicitly. They indicated that the optical properties of QDs are powerfully affected by the adjustable parameters and the magnetic field. In 2015, Guo et al. surveyed the optical properties of a QD under the applied hydrogenic impurity through studying the OACs and refractive index changes [21]. Their results revealed that the hydrogenic impurity affects strongly not only the peaks intensities but also the peaks positions of the OACs. Very recently, Haouari et al. investigated the hydrostatic pressure effects on the optical properties of spherical core/shell QDs [26]. They found that the binding energy, as well as the OACs in QDs are considerably affected by the core/shell radius, the impurity position, and the hydrostatic pressure. The main lack of these studies is that the e–p interaction has not been included.

It is well-known that the e–p scattering has a strong influence on the optical properties of low-dimensional semiconductor systems. That is the reason why the e-p interaction in such semiconductors has been scrutinized by a large mass of researchers in recent years. Using the compact-density-matrix method, Yu et al. investigated the effect of e–p scattering on the THG [27] and on the OACs [28] in quantum wires. Their results indicated that the e–p scattering led to the blue-shift of both THG and OACs peaks. The e–p interaction has also been demonstrated to make the increase in the intensities of all quantities describing the optical properties include the refractive index changes, the OACs [29], as well as the SHG and the THG [30] in a modified Gaussian QD. When surveying the effect of the e–p scattering on the optical properties of asymmetrical semi-exponential quantum wells, Xiao et al. [31] revealed that the optical rectification coefficient peaks have been enhanced and given blue-shift if the electron–LO-phonon interaction has been taken into account. In all these works, the optical properties have been studied taking account only one-photon process, while the two-photon absorption process has not been concerned.

In recent works [32–35], we have studied the contribution of the two-photon process to the OACs and the FWHM. The two-photon process has been indicated to give a remarkable addition to the total OACs as well as to the FWHM in comparison with the one-photon process. Note that, in the mentioned papers, the e–p interaction has been included in our calculations. However, the role of two-photon process in surveying the optical absorption in QDs is still insufficient, especially in the case of an induced-magnetic field. In this work, we scrutinize the optical absorption properties of QDs when the magnetic field is included, namely magneto-optical absorption. The two-photon process as well as the e–p scattering will also be taken into account in this work. Our paper is organized as follows: In Section 2, we brief the basic formulation for quantum dot model. The analytical expression for the magneto-optical absorption coefficient is presented in Section 3. The numerical results and discussion are performed in Section 4. Finally, conclusions are presented in Section 5.

2. Basic formulation for the QDs model

We examine a model of a QD, where the confinement of electrons in the z-direction is characterized by a triangular potential presented by Fang and Howard [36], where we assume that electron only occupies the lowest subband with energy E_{0z}. For the y-direction, the confinement is modeled by a parabolic potential of frequency ω_y, and the confinement in the x-direction is the infinite square potential, i.e., $V(x) = 0$ when $0 \le x \le L_x$ and $V(x) = \infty$ in other cases. When a static magnetic field of strength B is applied to the z-direction of the system, i.e., $\mathbf{B} = (0, 0, B)$, the Hamiltonian of one-electron reads

$$\mathcal{H} = \frac{1}{2m^*}(\mathbf{p}+|e|\mathbf{A})^2 + \frac{1}{2}m^*\omega_y^2 y^2 + V_0(z). \tag{1}$$

Here, $m^* = 0.067m_0$ [37] is the electron effective mass, $\mathbf{p}$ is the electron momentum operator, e is the electron charge, and $\mathbf{A} = (-By, 0, 0)$ is the vector potential. The eigenfunctions of Eq. (1) are given as

$$|\lambda\rangle = |N, n, 0\rangle = \sqrt{\frac{2}{L_x}}\sin\frac{n\pi x}{L_x}\phi_N(y - y_0)\psi_0(z), \tag{2}$$

where $N(= 0, 1, 2, \ldots)$ denotes the Landau level index, L_x and $n(= 1, 2, \ldots)$ are the normalized length and the electronic subband index in the x-direction, respectively. $\phi_N(y - y_0)$ denotes the harmonic-oscillator wave functions with $y_0 = -\widetilde{b}\widetilde{\alpha}_c{}^2 k_x$, in which, $\widetilde{b} = \omega_c/\widetilde{\omega}_c$, $\widetilde{\alpha}_c = (\hbar/m^*\widetilde{\omega}_c)^{1/2}$ being the renormalized magnetic length of the ground-state electron orbit, k_x presents the wave vector in the x-direction, $\widetilde{\omega}_c = (\omega_c^2 + \omega_y^2)^{1/2}$ denoting the renormalized cyclotron frequency with $\omega_c = eB/m^*$. The corresponding eigenvalues are given as

$$E_\lambda = E_{N,n,0} = \left(N + \frac{1}{2}\right)\hbar\widetilde{\omega}_c + \frac{n^2\pi^2\hbar^2}{2\widetilde{m}^*L_x^2} + E_{0z}, \tag{3}$$

where $\widetilde{m}^* = m^*\widetilde{\omega}_c^2/\omega_y^2$ is the renormalized mass related to the effective mass m^*. According to previous works [38,39], $\psi_0(z)$ in Eq. (2) is taken in the usual form of the variational wave function, i.e.,

$$\psi_0(z) = \xi_0^{3/2} z e^{-\xi_0 z/2} \tag{4}$$

where $\xi_0 = 3/\langle L_z\rangle$, with $\langle L_z\rangle$ being the average thickness in the z-direction.

3. Expression for the magneto-optical absorption coefficient

We now study the magneto-optical absorption properties of a QD model by considering the expression for the MOAC. The expression for MOAC was first presented to perform in quantum wells [35]; then it was developed and applied successfully in MoS_2 monolayer system [40] as well as in quantum wells [41,42]. Note that although the theory for the MOAC is established to perform in two-dimensional systems, this expression is general and can be applied in other systems even in one-dimensional QDs. The expression for the MOAC is given as follows [40]

$$K(\Omega) = \frac{1}{V_0(I/\hbar\Omega)} \sum_{\lambda,\lambda'} f_\lambda (1 - f_{\lambda'}) \mathcal{W}^{\pm}_{\lambda,\lambda'}. \tag{5}$$

Here, we mark the symbols as they were presented in Ref. [40]: I is the incident optical intensity of energy $\hbar\Omega$, V_0 is the system volume, and $f_\lambda = f_{N,n,0} = \left[e^{(E_{N,n,0}-E_F)/(k_BT)} + 1\right]^{-1}$ is Fermi distribution function for λ-state, in which E_F is the Fermi level, k_B is the Boltzmann constant, and T is the absolute temperature. The expression for the $f_{\lambda'}$ is expressed in the same form, but replace $E_{N,n,0}$ by $E_{N',n',0}$. The transition matrix element, $W^{\pm}_{\lambda,\lambda'}$, including p-photon process [43,44], is given as follows [40]

$$\begin{aligned} \mathcal{W}^{\pm}_{\lambda,\lambda'} &= \frac{2\pi}{\hbar^3\Omega^2} \sum_{\mathbf{q}} \sum_{p=1}^{\infty} |\mathcal{M}^{\pm}_{\lambda,\lambda'}|^2 |\mathcal{M}^{\text{rad}}_{\lambda,\lambda'}|^2 \\ &\times \frac{(\alpha_0 q_\perp)^{2p}}{(p!)^2 2^{2p}} \delta(E_{\lambda'} - E_\lambda \pm \hbar\omega_0 - p\hbar\Omega). \end{aligned} \tag{6}$$

Here, the plus and minus signs mention to the emission and absorption processes of one LO-phonon, respectively, α_0 is the dressing parameter. In Eq. (6), $\mathcal{M}^{\pm}_{\lambda,\lambda'}$ is the matrix element part due to e–p scattering, which is expressed as follows

$$|\mathcal{M}^{\pm}_{\lambda,\lambda'}|^2 = \frac{4\pi e^2 \chi^* \hbar\omega_0}{\epsilon_0 V_0 q^2} |J_{00}(q_z)|^2 |J_{\text{NN}'}(u)|^2 N_0^{\pm} \delta_{n,n'}, \tag{7}$$

where $\chi^* = (1/\chi_\infty - 1/\chi_0)$ is the reduction dielectric constant with $\chi_\infty = 10.89$ and $\chi_0 = 13.18$ [37], $\mathbf{q} = (q_\perp, q_z)$ denotes the phonon wave vector with $q_\perp^2 = q_x^2 + q_y^2$, $N_0^{\pm} = N_0 + 0.5 \pm 0.5$ with $N_0 = \left[e^{\hbar\omega_0/(k_BT)} - 1\right]^{-1}$ referring the Bose factor, which presents the number of LO-phonon of energy $\hbar\omega_0 = 36.25$ meV, and [38]

$$|J_{\text{NN}'}(u)|^2 = \frac{N_{\min}!}{N_{\max}!} e^{-u} u^{N_{\max}-N_{\min}} \left[L_{N_{\min}}^{N_{\max}-N_{\min}}(u)\right]^2, \tag{8)(9}$$

where $u = \tilde{\alpha}_c^2(q_x^2 + \tilde{b}^2 q_y^2)/2$, $N_{max} = \max(N, N')$, $N_{min} = \min(N, N')$, and $L_N^M(u)$ are the associated Laguerre polynomials.

The summation over $\mathbf{q}$ in Eq. (6) is performed by using the transformation $\Sigma_{\mathbf{q}} \to (V_0/(2\pi)^3) \int q_\perp dq_\perp dq_z d\varphi$. Then, the integration over φ gives a factor 2π. With the wave function $\psi_0(z)$ presented in Eq. (4), the integration over q_z is given by Eq. (8) of Ref. [38]

$$\int_{-\infty}^{+\infty} \frac{|J_{00}(q_z)|^2}{q_\perp^2 + q_z^2} \mathrm{d}q_z = \frac{3\pi\xi_0}{8q_\perp^2} I(\zeta_0) = \frac{F_{00}}{q_\perp^2}, \tag{10}$$

where we have denoted $F_{00} = 3\pi\xi_0 I(\zeta_0)/8$, in which, $I(\zeta_0) = 1/(1+\zeta_0) + 1/(1+\zeta_0)^2 + 2\zeta_0^2/3(1+\zeta_0)^3$ with $\zeta_0 = \xi_0/q_\perp$. Because of the factor $I(\zeta_0)$, the integration over $q_\perp$ becomes unmanageable. To solve this problem, according to Vasilopoulos et al. [38], we replace the factor $q_\perp$ in $I(\zeta_0)$ by its average value $\langle q_\perp \rangle = (2/\tilde{\alpha}_c^2)^{1/2}$. This results in a useful approximation $u \approx \tilde{\alpha}_c^2 q_\perp^2/2$ which is operative for $\omega_y \le \omega_c/2$ and therefore the integration over $q_\perp$ i.e. over u could be solved analytically.

We assume that the electromagnetic field is polarized in the y-direction, using Eq. (2), the matrix element part for the electron-photon interaction, $\mathcal{M}^{\text{rad}}_{\lambda,\lambda'}$, in Eq. (6) yields

$$\mathcal{M}^{\text{rad}}_{\lambda,\lambda'} = \frac{e\Omega A_0}{2} \mathcal{B}_{\lambda,\lambda'}, \tag{11}$$

where A_0 is the maximum value of the electromagnetic wave's vector potential, and

$$\mathcal{B}_{\lambda,\lambda'} = [y_0 \delta_{N',N} + (\tilde{\alpha}_c/\sqrt{2})(\sqrt{N}\delta_{N',N-1} + \sqrt{N+1}\delta_{N',N+1})]\delta_{n,n'}. \tag{12}$$

Eq. (12) reveals that the transitions occur when the LL index is unchanged ($\Delta N = 0$) or is changed only one unit ($\Delta N = \pm 1$). This result is fitted well with that reported in graphene [45–47] and other graphene-like systems [48,49].

Using the above expressions and Eqs. (A1) and (A4) of Ref. [50] to calculate the integration over $q_\perp$, and considering up to the two-photon process, ($p = 1, 2$), Eq. (5) becomes

$$K(\Omega) = A(\omega_c, \Omega) \sum_{N,n} \sum_{N',n'} f_{N,n,0}(1 - f_{N',n',0}) |\mathcal{B}_{\lambda,\lambda'}|^2 (Q_1 + Q_2) \delta_{n,n'}, \tag{13}$$

where we have denoted

$$A(\omega_c, \Omega) = \frac{e^4 \chi^* \hbar\omega_0 F_{00}}{4V_0 n_r c \epsilon_0^2 \hbar^2 \Omega} \left(\frac{\alpha_0}{\tilde{\alpha}_c}\right)^2, \tag{14)(15)(16}$$

Here, n_r and c are the refractive index and the speed of light, respectively. The argument of delta functions

$$P_p^{\pm} = \Delta E \pm \hbar\omega_0 - p\hbar\Omega, \quad p = 1, 2, \tag{17}$$

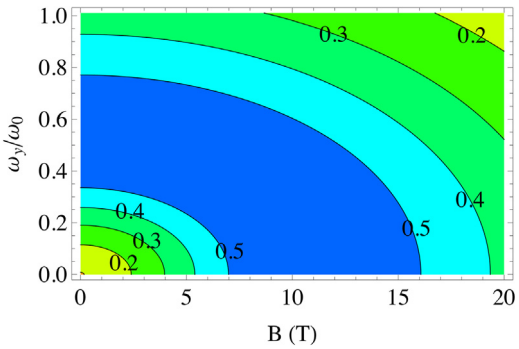

Fig. 1. Contour plot of the factor $f_{0,1,0}(1 - f_{1,1,0})$ versus the magnetic field (B) and the ratio ω_y/ω_0 at $T = 77$ K.

describes the selection rules with $\Delta E = E_{N',n',0} - E_{N,n,0}$ being the energy separation or threshold energy.

Because of their divergence when the arguments equal to zero, the delta functions in Eq. (13), as they appear in Eqs. (15) and (16), would be converted to the Lorentzians of width

$$(\gamma^{\pm})^2 = \sum_{\mathbf{q}} |\mathcal{M}^{\pm}_{\lambda,\lambda'}|^2. \tag{18}$$

Here, $\mathcal{M}^{\pm}_{\lambda,\lambda'}$ is the e–p interaction part of the matrix element shown in Eq. (7).

4. Numerical calculations and discussion

The following numerical results are calculated in a GaAs quantum dot. The material parameters used are [32–35,37,41]: $n_r = 3.2$, $\alpha_0 = 10$ nm, and the electron concentration $n_e = 3 \times 10^{16}$ cm^{-3} which leads to the Fermi level of $E_F = 14.18$ meV. The following results are obtained for $k_x = 0$, i.e., $y_0 = 0$, and for the transition between the two lowest states $|0, 1, 0\rangle$ and $|1, 1, 0\rangle$.

Because the factor $f_{0,1,0}(1 - f_{1,1,0})$ affects the magnitude of MOAC significantly, in Fig. 1, we show a contour plot of this factor as functions of magnetic field and ratio ω_y/ω_0. We can see that there is a maxima in the variation of both B and the ratio ω_y/ω_0. For $B = 0$, it first increases with the ratio ω_y/ω_0, achieves the maxima at $\omega_y/\omega_0 = 0.52$, then it starts to decrease when the ratio ω_y/ω_0 continues to rise further. The behavior is similar when we study the dependence of the factor on B, but the factor reaches its maximum value at $B = 10.79$ T.

The temperature and magnetic field variation of the contour plot of the factor $f_{0,1,0}(1 - f_{1,1,0})$ is shown in Fig. 2 for $\omega_y/\omega_0 = 0.2$. When $T \to 0$ K, all contours converge to two values of magnetic field of $B = 3.49$ T and 15.77 T. Therefore, with a fixed value of ratio $\omega_y/\omega_0 = 0.2$, it is better to study the MOAC in the range of magnetic field values between 3.49 T and 15.77 T. For higher values of temperature, this factor will decrease caused by the thermal spreading of the electron distribution functions when the temperature increases.

In order to understand the magnetic field effects on the magneto-optical properties, in Fig. 3, the photon energy dependence of MOAC is plotted for three values of B. The results are performed at $\omega_y/\omega_0 = 0.2$ and $T = 77$ K. There are two resonant peaks in each curves describing the one-photon (linear process, right-side peaks) and two-photon (nonlinear process, left-side peaks) absorption processes. These resonant peaks are formed by the transition of electrons between the two lowest states due to absorbing photons accompanied by the LO-phonon emission.

We can predict from the inset (right vertical axis) that the resonant peaks intensities are not monotonic functions of the magnetic field. When the strength of applied magnetic field become bigger, the linear peaks intensities firstly increase, reach the maximum

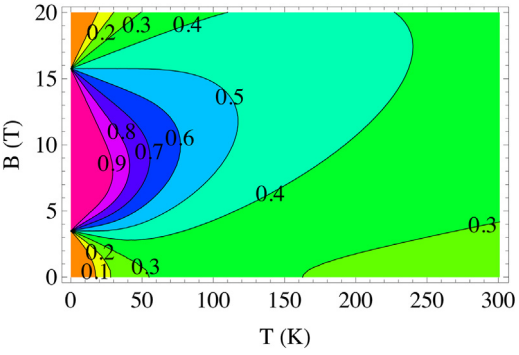

Fig. 2. Contour plot of the factor $f_{0,1,0}(1 - f_{1,1,0})$ versus the magnetic field and temperature at $\omega_y/\omega_0 = 0.2$.

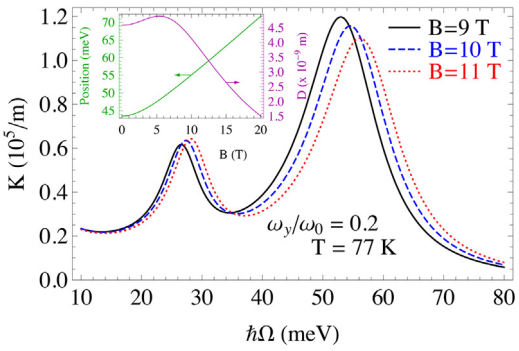

Fig. 3. MOAC as functions of photon energy for $B = 9$, 10, and 11 T. The inset illustrates the peaks' position due to the one-photon process (left vertical axis) and the factor $D = |\mathcal{B}_{\lambda,\lambda'}|^2 F_{00} f_{0,1,0}(1 - f_{1,1,0})$ (right vertical axis) due to the one-photon process as functions of magnetic field.

value at $B = 5.38$ T, and then start reducing if the magnetic field continues increases further. Meanwhile, the resonant peaks positions always shift towards the higher energy region (blue-shift) when the magnetic field is enhanced. The blue-shift of the resonant peaks with the rise of magnetic field, which is illustrated clearly in the inset (left vertical axis), is the result of the increase of the cyclotron energy ($\hbar\omega_c$), and so does the threshold energy ΔE. Besides, the reduction of the linear peaks is the consequence of the diminishing of factor $D = |\mathcal{B}_{\lambda,\lambda'}|^2 F_{00} f_{0,1,0}(1 - f_{1,1,0})$ when the magnetic field B increases from 9 to 11 Tesla.

For the two-photon (nonlinear) process, the magnetic field effects on MOAC is also supplemented by the addition of the factor $\widetilde{\alpha}_c^{-2}$ (see Eq. (16)). Therefore, under the change of magnetic field, there is a competition effect on the magnitude of the two-photon resonant peaks between two factors $\widetilde{\alpha}_c$ and D. The increase of the magnitude of the two-photon absorption peaks indicates that, in this case, the effect of the factor $\widetilde{\alpha}_c^{-2}$ is dominant in comparison with the influence of the factor D when the magnetic field increases.

Fig. 4 depicts the photon energy dependence of MOAC for several values of ratio ω_y/ω_0. The result shows that the effect of the ratio ω_y/ω_0 (or the confinement frequency) is very close to the magnetic field effect presented above in Fig. 3, i.e., when the ratio ω_y/ω_0 increases the peaks position give a blue-shift and the linear peaks intensities decrease. This familiar feature is the result of the fact that the dependence of MOAC on ω_y and B, entering through the cyclotron frequency ($\omega_c = eB/m^*$), are the same: the MOAC depends on these two factors through the renormalized cyclotron frequency $\widetilde{\omega}_c = (\omega_c^2 + \omega_y^2)^{1/2}$. The only different feature is that the factor D is a decreasing function of the ratio ω_y/ω_0 in the investigated region. This difference is derived from a choice of the magnetic field of $B = 10$ T, corresponding to the cyclotron energy of $\hbar\omega_c = 17.39$ meV which is much bigger than the confining energy $\hbar\omega_y = 0.2\,\hbar\,\omega_0 = 7.25$ meV. To illustrate this argument, we plot the factor D at $\hbar\omega_c = 0.2\,\hbar\,\omega_0$, corresponding to $B = 4.17$ T, as shown in the dashed-curve in the inset of Fig. 4. It is clear that in this case, the behavior of the factor D is close to that as illustrated in the inset of Fig. 3.

In Fig. 5, we show the photon energy dependence of the MOAC for distinct values of temperature at $\omega_y/\omega_0 = 0.2$ and $B = 10$ T. With the increase of temperature, the magnitude of the MOAC peaks reduces but their positions do not change. The reduction of the magnitude results from the decrease of the factor D while the maintaining of the position is the consequence of the temperature-independence of the threshold energy $\Delta E = E_{1,1,0} - E_{0,1,0}$, as shown in the inset of Fig. 5. Whereas the peaks' position due to the one-photon absorption process is given as $\hbar\Omega = \Delta E + \hbar\,\omega_0$, which is independent of temperature.

We now take into consideration the FWHM of the resonant peaks in two cases of one- and two-photon processes. We can see from Fig. 6 that FWHM appears as a nonlinear increasing function of magnetic field. This implies that the e–p scattering has a directly proportional relationship with magnetic field. However, unlike the $\sqrt{B}$-dependent FWHM in the quantum well models [32,51–53] and in graphene [54–58], in the quantum dot, the law of this feature is more complicated. The best-fit for the magnetic field dependence of FWHM is found to be: FWHM (meV) = $5.36 + 3.20(10 + B[\mathrm{T}]^2)^{1/4}$ for the one-photon process and

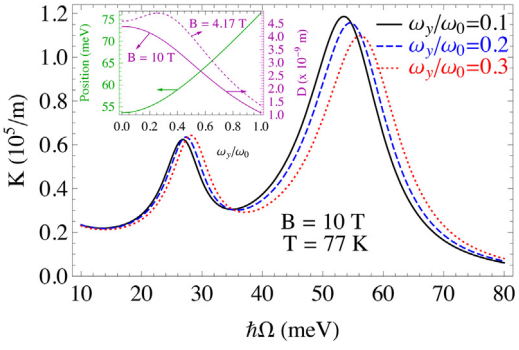

Fig. 4. MOAC as functions of photon energy for $\omega_y/\omega_0$0.1, 0.2 and 0.3. The inset illustrates the peaks' position due to the one-photon process (left vertical axis) and the factor $D = |\mathcal{B}_{\lambda,\lambda'}|^2 F_{00} f_{0,1,0}(1 - f_{1,1,0})$ (right vertical axis) due to one-photon process as functions of ω_y/ω_0.

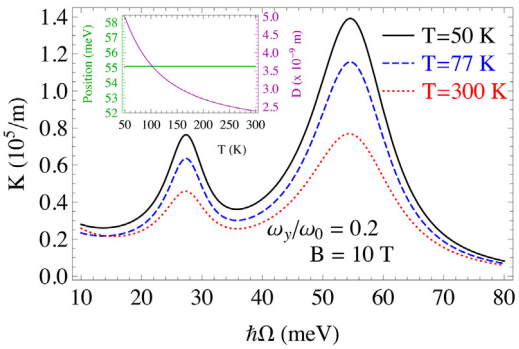

Fig. 5. MOAC as functions of photon energy for $T = 50$, 77, and 300 K. The inset illustrates the peaks' position due to the one-photon process (left vertical axis) and the factor $D = |\mathcal{B}_{\lambda,\lambda'}|^2 F_{00} f_{0,1,0}(1 - f_{1,1,0})$ (right vertical axis) due to one-photon absorption process as functions of temperature.

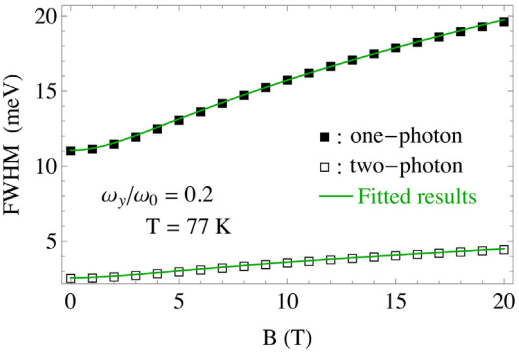

Fig. 6. FWHM as functions of the magnetic field.

FWHM (meV) $= 1.3 + 0.71(10 + B[\mathrm{T}]^2)^{1/4}$ for the two-photon one, respectively. These are probably new results. Besides, the values of FWHM in QDs clearly outweigh those in quantum wells. This implies that the e–p interaction in quantum dots is much more potent than that in quantum wells.

The dependence of the FWHM on the ratio ω_y/ω_0 is shown in Fig. 7. It is clear that the FWHM rises nonlinearly with the increasing ratio. Physically, when the ratio ω_y/ω_0 (or the confinement frequency ω_y) becomes bigger, the confinement effect will become more strengthened, leading to the enhance of the e–p scattering, and so does the FWHM. Quantitatively, we found the best-fit for the dependence of FWHM on this ratio as follows: FWHM (meV) $= 8.9 + 11.25[0.1 + (\omega_y/\omega_0)^2]^{1/4}$ for the one-photon process and FWHM (meV) $= 2.25 + 2.70[0.1 + (\omega_y/\omega_0)^2]^{1/4}$ the two-photon ones, respectively. We can see that these expressions are in the same form of that presented the dependence of FWHM on the magnetic field, because the expression of the renormalized cyclotron frequency, $\widetilde{\omega}_c = (\omega_c^2 + \omega_y^2)^{1/2}$, reveals that the roles of ω_c (or magnetic field B) and ω_y are equivalent.

Finally, in Fig. 8, the FWHM is found to extend non-linearly with the rising temperature caused by the thermal expanding FWHM, which is expressed quantitatively as the resulting of the electron–LO-phonon scattering as follows [59,60]: FWHM (meV) $= b_0 + b_T N_0$, where b_0 and b_T are the constants, which have the unit of energy, and N_0 is Bose distribution. From a fit to equation above, and using the expression for N_0 as presented in Section 3, we have determined the values for b_0 and b_T as: $b_0 = 15.76$

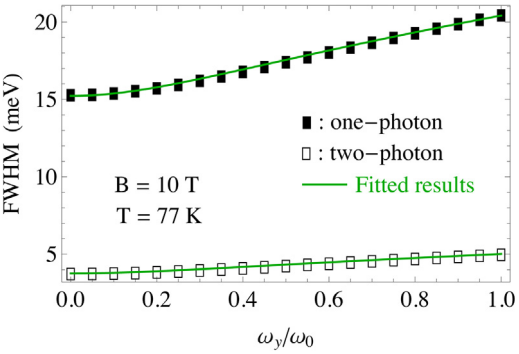

Fig. 7. FWHM as functions of the ratio ω_y/ω_0.

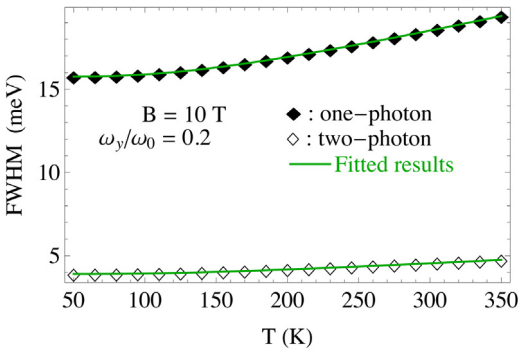

Fig. 8. FWHM as functions of the temperature.

(3.90) and $b_T = 8.45$ (1.97) for the one (two)-photon process as presented by the green lines in Fig. 8. We can see that they are fitted well qualitatively with the previous experimental report in multiple quantum well [59,60]. Besides, these value of b_0 and b_T are also higher than those in quantum well [41]. This result implies that the e–p interaction in quantum dots is more potent than that in quantum wells. Thus, the geometric confinement has a significant effect on the e–p interaction in such low-dimensional quantum systems.

5. Conclusions

We have scrutinized a study of the magneto-optical absorption in QDs in which the two-photon process has been taken into account. The numerical results are performed for GaAs materials. The optimized range of the magnetic field for studying MOAC and FWHM is from $B = 3.49$ T to $B = 15.77$ T. When the strength of magnetic field is enhanced, the magnitude of the linear peaks firstly increases, hits the maximum value at $B = 5.38$ T, and then starts reducing if the magnetic field continues increases further, while the magnitude of the nonlinear peaks is always enhanced, but the resonant peaks positions always shift towards high energy region. When the temperature increases the peaks intensities are reduced but their positions do not change.

The FWHM in QDs is much larger than that in quantum wells and powerfully depends on the magnetic field, the temperature and the confinement frequency: FWHM is found to rise with confinement frequency, to extend non-linearly with the rising temperature caused by the thermal expanding FWHM. For magnetic field dependence of FWHM we expect the fitted results FWHM (meV) $= 5.36 + 3.20(10 + B[\mathrm{T}]^2)^{1/4}$ for the one-photon process and FWHM (meV) $= 1.3 + 0.71(10 + B[\mathrm{T}]^2)^{1/4}$ for the two-photon one, respectively. In our knowledge, these are new results, and it is necessary to have an experiment work to test their validities. Our results also reveal that the geometric confinement has a significant effect on the e–p interaction in such low-dimensional quantum systems. We believe that the obtained results may promote novel applications of the quantum confinement effect at nanoscales in nano-optoelectronic devices.

Acknowledgment

This research is supported by Quang Binh University under Grant Number CS.10.2018.

References

[1] E. Leobandung, L. Guo, S.Y. Chou, Appl. Phys. Lett. 67 (1995) 2338.
[2] G.W. Walker, V.C. Sundar, C.M. Rudzinski, A.W. Wun, M.G. Bawendi, D.G. Nocera, Appl. Phys. Lett. 83 (2003) 3555.
[3] S. Chaudhary, M. Ozkan, W.C.W. Chan, Appl. Phys. Lett. 84 (2004) 2925.
[4] M. Troccoli, A. Belyanin, F. Capasso, E. Cubukcu, D.L. Sivco, A.Y. Cho, Nature 433 (2005) 845.
[5] S. Baskoutas, E. Paspalakis, A.F. Terzis, Phys. Rev. B 74 (2006) 153306.
[6] I. Karabulut, H. Safak, M. Tomak, Solid State Commun. 135 (2005) 735.
[7] A. Vella, F. Vurpillot, B. Gault, A. Menand, B. Deconihout, Phys. Rev. B 73 (2006) 165416.
[8] S. Baskoutas, E. Paspalakis, A.F. Terzis, J. Phys.: Condens. Matter 19 (2007) 395024.
[9] T. Brunhes, P. Boucaud, S. Sauvage, A. Lemaître, J.-M. Gérard, F. Glotin, R. Prazeres, J.-M. Ortega, Phys. Rev. B 61 (2000) 5562.
[10] U. Gubler, C. Bosshard, Phys. Rev. B 61 (2000) 10702.
[11] A. Majumdar, D. Gerace, Phys. Rev. B 87 (2013) 235319.
[12] M. Jacobsohn, U. Banin, J. Phys. Chem. B 104 (2000) 1.
[13] O. Malis, A. Belyanin, C. Gmachl, D.L. Sivco, M.L. Peabody, A.M. Sergent, A.Y. Cho, Appl. Phys. Lett. 84 (2004) 2721.
[14] S. Campione, A. Benz, M.B. Sinclair, F. Capolino, I. Brener, Appl. Phys. Lett. 104 (2014) 131104.
[15] S. Sauvage, P. Boucaud, F. Glotin, R. Prazeres, J.-M. Ortega, A. Lemaître, J.-M. Gérard, V. Thierry-Mieg, Phys. Rev. B 59 (1999) 9830.
[16] G. Wang, K. Guo, J. Phys.: Condens. Matter 13 (2001) 8197.
[17] G. Wang, Phys. Rev. B 72 (2005) 155329.
[18] S. Sakiroglu, F. Ungan, U. Yesilgul, M. Mora-Ramos, C. Duque, E. Kasapoglu, H. Sari, I. Sokmen, Phys. Lett. A 376 (2012) 1875.
[19] K.-X. Guo, B. Xiao, Y. Zhou, Z. Zhang, J. Opt. 17 (2015) 035505.
[20] I. Karabulut, S. Baskoutas, J. Appl. Phys. 103 (2008) 073512.
[21] K. Guo, Z. Zhang, S. Mou, B. Xiao, J. Opt. 17 (2015) 055504.

[22] B. Çakir, Y. Yakar, A. Özmen, Physica B 510 (2017) 86.
[23] A. Vartanian, A. Asatryan, L. Vardanyan, Superlattices Microstruct. 103 (2017) 205.
[24] L. Bouzaiene, H. Alamri, L. Sfaxi, H. Maaref, J. Alloys Compd. 655 (2016) 172.
[25] G. Liu, K. Guo, H. Hassanabadi, L. Lu, Physica B 407 (2012) 3676.
[26] M. El Haouari, A. Talbi, E. Feddi, H. El Ghazi, A. Oukerroum, F. Dujardin, Opt. Commun. 383 (2017) 231.
[27] Y.-B. Yu, K.-X. Guo, S.-N. Zhu, Physica E 27 (2005) 62.
[28] Y.-B. Yu, S.-N. Zhu, K.-X. Guo, Solid State Commun. 139 (2006) 76.
[29] R. Khordad, H. Bahramiyan, Opt. Quantum. Electron. 47 (2015) 2727.
[30] R. Khordad, H. Bahramiyan, Superlattices Microstruct. 76 (2014) 163.
[31] B. Xiao, K. Guo, S. Mou, Z. Zhang, Superlattices Microstruct. 69 (2014) 122.
[32] H.V. Phuc, N.N. Hieu, L. Dinh, T.C. Phong, Opt. Commun. 335 (2015) 37.
[33] H.V. Phuc, J. Phys. Chem. Solids 82 (2015) 36.
[34] L.V. Tung, H.V. Phuc, Superlattices Microstruct. 89 (2016) 288.
[35] H.V. Phuc, N.D. Hien, L. Dinh, T.C. Phong, Superlattices Microstruct. 94 (2016) 51.
[36] F.F. Fang, W.E. Howard, Phys. Rev. Lett. 16 (1966) 797.
[37] S. Adachi, J. Appl. Phys. 58 (1985) R1.
[38] P. Vasilopoulos, P. Warmenbol, F.M. Peeters, J.T. Devreese, Phys. Rev. B 40 (1989) 1810.
[39] J.Y. Ryu, R.F. O'Connell, Phys. Rev. B 48 (1993) 9126.
[40] C.V. Nguyen, N.N. Hieu, N.A. Poklonski, V.V. Ilyasov, L. Dinh, T.C. Phong, L.V. Tung, H.V. Phuc, Phys. Rev. B 96 (2017) 125411.
[41] L.V. Tung, P.T. Vinh, H.V. Phuc, Physica B 539 (2018) 117.
[42] K.D. Pham, L. Dinh, P.T. Vinh, C.A. Duque, H.V. Phuc, C.V. Nguyen, Superlattices Microstruct. 120 (2018) 738.
[43] W. Xu, R.A. Lewis, P.M. Koenraad, C.J.G.M. Langerak, J. Phys.: Condens. Matter 16 (2004) 89.
[44] W. Xu, Phys. Rev. B 57 (1998) 12939.
[45] V. Gusynin, S. Sharapov, J. Carbotte, Phys. Rev. Lett. 98 (2007) 157402.
[46] M. Koshino, T. Ando, Phys. Rev. B 77 (2008) 115313.
[47] C.V. Nguyen, N.N. Hieu, C.A. Duque, N.A. Poklonski, V.V. Ilyasov, N.V. Hieu, L. Dinh, Q.K. Quang, L.V. Tung, H.V. Phuc, Opt. Mater. 69 (2017) 328.
[48] C.V. Nguyen, N.N. Hieu, C.A. Duque, D.Q. Khoa, N.V. Hieu, L.V. Tung, H.V. Phuc, J. Appl. Phys. 121 (2017) 045107.
[49] C.V. Nguyen, N.N. Hieu, D. Muoi, C.A. Duque, E. Feddi, H.V. Nguyen, L.T.T. Phuong, B.D. Hoi, H.V. Phuc, J. Appl. Phys. 123 (2018) 034301.
[50] P. Vasilopoulos, Phys. Rev. B 33 (1986) 8587.
[51] M.P. Chaubey, C.M. Van Vliet, Phys. Rev. B 34 (1986) 3932.
[52] H.V. Phuc, N.T.T. Thao, L. Dinh, T.C. Phong, J. Phys. Chem. Solids 75 (2014) 300.
[53] H.V. Phuc, D.Q. Khoa, N.V. Hieu, N.N. Hieu, Optik 127 (2016) 10519.
[54] G. Li, A. Luican, E.Y. Andrei, Phys. Rev. Lett. 102 (2009) 176804.
[55] M. Orlita, C. Faugeras, P. Plochocka, P. Neugebauer, G. Martinez, D.K. Maude, A.-L. Barra, M. Sprinkle, C. Berger, W.A. de Heer, M. Potemski, Phys. Rev. Lett. 101 (2008) 267601.
[56] H.V. Phuc, N.N. Hieu, Opt. Commun. 344 (2015) 12.
[57] H.V. Phuc, L. Dinh, Mater. Chem. Phys. 163 (2015) 116.
[58] H.V. Phuc, Superlattices Microstruct. 88 (2015) 518.
[59] D.A.B. Miller, D.S. Chemla, D.J. Eilenberger, P.W. Smith, A.C. Gossard, W.T. Tsang, Appl. Phys. Lett. 41 (1982) 679.
[60] D. Gammon, S. Rudin, T.L. Reinecke, D.S. Katzer, C.S. Kyono, Phys. Rev. B 51 (1995) 16785.